Research Article | Vol. 9, No. 9 | 1 Sep 2018 | BIOMEDICAL OPTICS EXPRESS 4459

Biomedical Optics EXPRESS

Rapid and in situ optical detection of trace lithium in tissues

IRFAN AHMED,[1,2] JINGWEI YANG,[1] ALAN WING LUN LAW,[1] FRANCIS A. M. MANNO,[1] RAFAY AHMED,[1] YANPENG ZHANG,[3] AND CONDON LAU[1,*]

[1]*Department of Physics, City University of Hong Kong, Hong Kong SAR, China*
[2]*Department of Electrical Engineering, Sukkur IBA University, Sukkur 65200, Pakistan*
[3]*Key Laboratory for Physical Electronics and Devices of the Ministry of Education and Shaanxi Key Lab of Information Photonic Technique, Xi'an Jiaotong University, Xi'an 710049, China*
*condon.lau@cityu.edu.hk

Abstract: Lithium-based medications are used successfully to treat many mental disorders, including bipolar disorder and Alzheimer's disease. However, the therapeutic mechanisms are not well characterized due to limitations in detecting lithium in organs and cells. This limits the ability to improve lithium-based treatments. To address this need, laser-induced breakdown spectroscopy (LIBS) is developed for the rapid and in situ detection of lithium in biological tissues. Pronounced lithium emissions are observed at 670.7nm from the rat thyroid, salivary, and mammary glands when lithium is administered orally. Calcium, carbon, magnesium, sodium, potassium, and iodine emissions are also observed. The lithium emission intensity is positively correlated with tissue lithium concentration, which is ~1ppm. The limit of detection for lithium is determined to be ~0.1ppm. Thyroid lithium intensity increases while iodine intensity decreases. The reduced intrathyroidal iodine following treatment likely impairs hormone production. Further, the presence of lithium in the salivary and mammary glands makes these glands the likely conduits for lithium to enter the saliva and breast milk, respectively. LIBS is well suited for characterizing the distribution of lithium, and other elements, across the body. This optical method can potentially be adapted for use in vivo and in humans.

© 2018 Optical Society of America under the terms of the OSA Open Access Publishing Agreement

OCIS codes: (300.6365) Spectroscopy, laser induced breakdown; (170.6935) Tissue characterization.

References and links

1. C. L. Murray, "The Global Burden of Disease: A comprehensive assessment of mortality and disability from diseases, injuries, and risk factors in 1990 and projected to 2020," Harvard University Press on behalf of the World Health Organization, Harvard School of Public Health, and World Bank (Harvard, 1996).
2. M. W. Jann, "Diagnosis and treatment of bipolar disorders in adults: a review of the evidence on pharmacologic treatments," Am. Health Drug Benefits **7**(9), 489–499 (2014).
3. R. W. Kupka, W. A. Nolen, R. M. Post, S. L. McElroy, L. L. Altshuler, K. D. Denicoff, M. A. Frye, P. E. Keck, Jr., G. S. Leverich, A. J. Rush, T. Suppes, C. Pollio, and H. A. Drexhage, "High rate of autoimmune thyroiditis in bipolar disorder: lack of association with lithium exposure," Biol. Psychiatry **51**(4), 305–311 (2002).
4. C. J. Phiel, C. A. Wilson, V. M.-Y. Lee, and P. S. Klein, "GSK-3α regulates production of Alzheimer's disease amyloid-β peptides," Nature **423**(6938), 435–439 (2003).
5. M. Hong, D. C. Chen, P. S. Klein, and V. M. Lee, "Lithium reduces tau phosphorylation by inhibition of glycogen synthase kinase-3," J. Biol. Chem. **272**(40), 25326–25332 (1997).
6. S. Rej, K. Shulman, and N. Herrmann, "Long-term effects of lithium on renal function," Lancet **386**(10007), 1943–1944 (2015).
7. T. K. Creson, P. J. Monaco, E. M. Rasch, A. H. Hagardorn, and K. E. Ferslew, "Capillary ion analysis of lithium concentrations in biological fluids and tissues of Poecilia (teleost)," Electrophoresis **19**(16-17), 3018–3021 (1998).
8. J. Lichtinger, R. Gernhäuser, A. Bauer, M. Bendel, L. Canella, M. Graw, R. Krücken, P. Kudejova, E. Mützel, S. Ring, D. Seiler, S. Winkler, K. Zeitelhack, and J. Schöpfer, "Position sensitive measurement of lithium traces in brain tissue with neutrons," Med. Phys. **40**(2), 023501 (2013).
9. G. Zanni, W. Michno, E. Di Martino, A. Tjärnlund-Wolf, J. Pettersson, C. E. Mason, G. Hellspong, K. Blomgren, and J. Hanrieder, "Lithium Accumulates in Neurogenic Brain Regions as Revealed by High Resolution Ion Imaging," Sci. Rep. **7**(1), 40726 (2017).
10. S. Natarajan and H. C. Bajaj, "Recovered materials from spent lithium-ion batteries (LIBs) as adsorbents for dye

#323292 https://doi.org/10.1364/BOE.9.004459
Journal © 2018 Received 20 Feb 2018; revised 9 Aug 2018; accepted 17 Aug 2018; published 27 Aug 2018

Biomedical Optics EXPRESS

removal: Equilibrium, kinetics and mechanism," J. Environ. Chem. Eng. **4**(4), 4631–4643 (2016).
11. J. Kaiser, K. Novotny, M. Z. Martin, A. Hrdlica, R. Malina, M. Hartl, V. Adam, and W. H. Weinberg, "Trace elemental analysis by laser-induced breakdown spectroscopy—Biological applications," Surf. Sci. Rep. **67**(11-12), 233–243 (2012).
12. D. W. Hahn and N. Omenetto, "Laser-induced breakdown spectroscopy (LIBS), Part II: review of instrumental and methodological approaches to material analysis and applications to different fields," Appl. Spectrosc. **66**(4), 347–419 (2012).
13. V. K. Unnikrishnan, K. Alti, R. Nayak, R. Bernard, N. Khetarpal, V. B. Kartha, C. Santhosh, G. P. Gupta, and B. M. Suri, "Optimized LIBS setup with echelle spectrograph-ICCD system for multi-elemental analysis," J. Instrum. **5**(04), P04005 (2010).
14. X.-Y. Liu and W.-J. Zhang, "Recent developments in biomedicine fields for laser induced breakdown spectroscopy," J. Biomed. Sci. Eng. **1**(03), 147–151 (2008).
15. S. H. C. Manno, F. A. M. Manno, I. Ahmed, R. Ahmed, L. Shu, L. Li, S. Xu, F. Xie, V. W. Li, J. Ho, S. H. Cheng, and C. Lau, "Spectroscopic examination of enamel staining by coffee indicates dentin erosion by sequestration of elements," Talanta **189**, 550–559 (2018).
16. C. Fabre, M.-C. Boiron, J. Dubessy, A. Chabiron, B. Charoy, and T. Martin Crespo, "Advances in lithium analysis in solids by means of laser-induced breakdown spectroscopy: an exploratory study," Geochim. Cosmochim. Acta **66**(8), 1401–1407 (2002).
17. D. A. Cremers, A. Beddingfield, R. Smithwick, R. C. Chinni, C. R. Jones, B. Beardsley, and L. Karch, "Monitoring Uranium, Hydrogen, and Lithium and Their Isotopes Using a Compact Laser-Induced Breakdown Spectroscopy (LIBS) Probe and High-Resolution Spectrometer," Appl. Spectrosc. **66**(3), 250–261 (2012).
18. A. M. Leung and L. E. Braverman, "Consequences of excess iodine," Nat. Rev. Endocrinol. **10**(3), 136–142 (2014).
19. G. S. Senesi, M. Dell'Aglio, R. Gaudiuso, A. De Giacomo, C. Zaccone, O. De Pascale, T. M. Miano, and M. Capitelli, "Heavy metal concentrations in soils as determined by laser-induced breakdown spectroscopy (LIBS), with special emphasis on chromium," Environ. Res. **109**(4), 413–420 (2009).
20. W. V. Welshons, K. S. Engler, J. A. Taylor, L. H. Grady, and E. M. Curran, "Lithium-stimulated proliferation and alteration of phosphoinositide metabolites in MCF-7 human breast cancer cells," J. Cell. Physiol. **165**(1), 134–144 (1995).
21. R. A. Merendino, G. Mancuso, F. Tomasello, D. Gazzara, V. Cusumano, S. Chillemi, P. Spadaro, and M. Mesiti, "Effects of lithium carbonate on cytokine production in patients affected by breast cancer," J. Biol. Regul. Homeost. Agents **8**(3), 88–91 (1994).
22. D. L. Bogen, D. Sit, A. Genovese, and K. L. Wisner, "Three cases of lithium exposure and exclusive breastfeeding," Arch. Women Ment. Health **15**(1), 69–72 (2012).
23. W. C. Baha Zantour and W. Chebbi, "Lithium Treatment and Thyroid Disorders," Journal of Thyroid Disorders & Therapy **03**, 143 (2014).
24. C. Paton, T. R. Barnes, A. Shingleton-Smith, R. H. McAllister-Williams, J. Kirkbride, P. B. Jones, and S. McIntyre; POMH-UK project team, "Lithium in bipolar and other affective disorders: prescribing practice in the UK," J. Psychopharmacol. (Oxford) **24**(12), 1739–1746 (2010).
25. I. Ahmed, R. Ahmed, J. Yang, A. W. L. Law, Y. Zhang, and C. Lau, "Elemental analysis of the thyroid by laser induced breakdown spectroscopy," Biomed. Opt. Express **8**(11), 4865–4871 (2017).
26. A. W. L. Law, R. Ahmed, T. W. Cheung, C. Y. Mak, and C. Lau, "In situ cellular level Raman spectroscopy of the thyroid," Biomed. Opt. Express **8**(2), 670–678 (2017).
27. N. Serdarević, F. Kozjek, and I. Malesic, "Saliva and serum lithium monitoring in hospitalized patients and possibility to replace serum to saliva," Bosn. J. Basic Med. Sci. **6**(4), 32–35 (2008).

1. Introduction

Bipolar disorder and Alzheimer's disease are two widely prevalent mental disorders that significantly affect the patient's quality of life. According to the World Health Organization, bipolar disorder is among the ten leading causes of reduction in disability-adjusted life years [1]. The disease prevalence is about 2.4% and health care systems in developed countries have not adequately responded to as many as 50% of the patients. In the United States, the lifetime prevalence of bipolar disorder in adults is approximately 4%, and its management has been estimated to cost $150 billion [2]. Lithium-based psychotherapy medication is considered one of the most effective treatments of bipolar disorder [3] and for prevention of Alzheimer's [4,5]. Lithium significantly reduces depression and mania, the main symptoms of bipolar disorder. Lithium treatment also significantly reduces suicide attempts and suicide deaths compared with other drugs [3]. However, lithium comes with side-effects. Lithium is associated with thyroid and overall endocrine dysfunction and has poorly characterized adverse effects on the kidneys [6]. Further, the mechanisms through which lithium impacts mental disorders is not well understood. The poor characterization of such effects is due in

Biomedical Optics EXPRESS

large part to difficulties in detecting trace levels (parts-per-million, ppm, and below) of lithium in biological samples.

A method for detecting trace lithium in a biology lab has to be sensitive to trace levels in small samples weighing milligrams or less. The reason is, biomedical research is often performed on the cells and tissues of small animals. Even larger human specimens should preferably not be entirely consumed by the method. Further, the method should involve relatively straight forward sample preparation that preserves the microstructure and biochemistry as much as possible. Also, equipment cost and size are preferably low to encourage wide use. These specifications are not well met by conventional elemental analysis methods such as x-ray fluorescence (XRF) or inductively coupled plasma mass spectroscopy (ICP-MS). XRF is relatively insensitive to lithium and acid digestion ICP-MS typically requires larger samples. Lithium has been detected in blood plasma by capillary ion analysis [7], and in brain tissue by neutron capture reaction [8] and high resolution ion imaging [9]. These techniques are laborious, expensive, and not well suited to rapid and in situ analysis of biological samples.

Laser-induced breakdown spectroscopy (LIBS) is an optical elemental analysis method that is highly sensitive to light elements such as lithium [10,11]. LIBS employs a high intensity laser pulse to ablate a small volume (μm^3) of the sample [12]. This leads to an optical emission spectrum that is characteristic of the elements in the sample along with their concentrations. LIBS instrumentation is relatively compact and inexpensive, measurements can be performed in standard atmosphere, and sample preparation is relatively straight forward. Further, LIBS can analyze all elements simultaneously and measurements can be completed in seconds, even with small sample volumes [13]. Due to the fine sampling of LIBS, it can be applied for rapid and in situ analysis of small organs and cells. Based on these properties, LIBS has been applied to biomedical applications [14,15]. LIBS has been employed to examine lithium in non-biological applications such as geology [16], nuclear forensics [17], alloy detection, and in used lithium ion batteries [10].

In this article, we develop LIBS to detect lithium, along with other elements, in the thyroid, salivary, and mammary glands of rats after treating them with lithium medication. The thyroid is an important endocrine gland located in the neck. It is primarily responsible for secreting the hormones triiodothyronine (T_3) and thyroxine (T_4), which regulate metabolism [18]. Having the correct intrathyroidal levels of important elements, such as iodine, is essential for the production of T_3 and T_4. Moreover, the concentrations of such elements in the salivary and mammary glands are also important for their functions, such as secreting saliva and breast milk. This study analyzes the glands at the organ level, but long-term, LIBS can potentially perform cellular level lithium analysis across a range of tissues. This will make LIBS a very important method for lithium biodistribution studies.

The structure of this article is as follows. The materials and methods section describes the LIBS setup, sample preparation, and data analysis. Two types of samples are prepared. The first sample type is thyroid, salivary, and mammary glands from subjects treated with lithium orally, modeling medical treatment. The second are thyroids harvested from untreated subjects and immersed in lithium solution. These samples are for validating that measured LIBS emission lines are due to lithium in the sample and for calibrating the emission intensities to lithium concentration. The results and discussion section presents LIBS spectra measured from the samples and how the lithium emission line, along with that of other elements, depend on lithium level.

2. Material and methods

2.1 Animal subjects

The animal research protocol of this study was evaluated and approved by the relevant ethics committees of the City University of Hong Kong, the University of Hong Kong, and the Department of Health of the Hong Kong Special Administrative Region. Male Sprague

Biomedical Optics EXPRESS

Dawley (SD) rats (N = 45, 250-300 g) and female rats (N = 10, 250-300 g) were employed. Subjects were provided by the AAALAC accredited Laboratory Animal Unit of the University of Hong Kong. Five subjects were housed in one cage under a constant temperature of 25 °C and humidity of 60 to 70% at the Laboratory Animal Research Unit of the City University of Hong Kong. Subjects were housed in 12/12 hour light/dark cycles and had access to regular chow food and drinking water. Subjects were acclimated to the housing environment for at least one day prior to experimentation.

The male subjects were divided into an untreated group (N = 30) and three groups receiving lithium treatment (N = 5 each). Twenty five of the untreated subjects were sacrificed upon entry. Their thyroids were harvested and immersed in lithium solutions of varying concentration. The thyroids from the remaining five untreated subjects (N = 5) formed the untreated group and were control subjects. In this manuscript, control subjects will typically be referred to as controls. The treated subjects were administered lithium through drinking water for 14, 28, or 42 days before being sacrificed and their thyroids and salivary glands harvested. The controls drank regular drinking water. The female subjects were divided into two groups. Five of the subjects received lithium. The other five were untreated controls. Treated subjects were administered lithium for 42 days.

2.2 Experimental setup and data acquisition

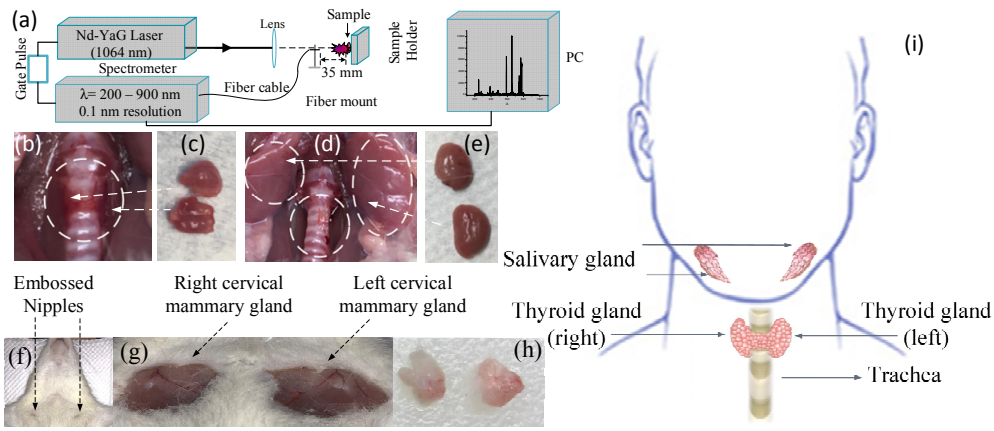

Fig. 1. (a) Schematic diagram of the laser-induced breakdown spectroscopy (LIBS) setup. The laser pulse is focused by the lens onto the sample. The ablated portion of the sample emits light, which is collected by the fiber and channeled to the spectrometer. The setup is controlled by a personal computer (PC), which triggers both the laser and the spectrometer and displays the spectrum. (b) The portion of the neck around the trachea where the thyroid is located (circled). (c) The harvested thyroid with two lobes. (d) The same portion of the neck after the thyroid was removed and the upper left and right circles indicate the salivary glands. (e) The harvested left and right salivary glands. (f) The portion of the chest from a female subject showing the embossed nipples. (g) Same portion of the chest showing the nipples after shaving. (h) The harvested left and right cervical mammary glands. (i) The anatomical illustration of the thyroid and salivary glands in humans.

Figure 1(a) shows the setup of LIBS. The 1064 nm pulsed laser (CFR200, Quantel) emitted 8 ns, 200 mJ pulses focused to a 10 µm spot on the sample. The optical emission from the ablated tissue was collected by a six channel fiber bundle (2000 µm diameter) positioned 35 mm from the focus and at 45° from the laser beam. The fibers relayed light to six spectrometers spanning 200 – 900 nm with 0.1 nm resolution (MX2500 + , Ocean Optics). The spectrometer was triggered to acquire 1.9 µs after laser firing and with integration time of 1 ms. LIBS was performed in standard air atmosphere. The computer processed the spectra acquired by the spectrometers and produced the graphical presentation of spectral intensity against the corresponding wavelength.

Biomedical Optics EXPRESS

Before data acquisition, the spectrometer was calibrated using the argon gas and mercury lamp (PhyWe) spectra. The argon and mercury spectra were matched with spectral lines available in the Atomic Spectra Database of the National Institute of Standards and Technology. One day prior to LIBS, samples were transferred from −80 °C and stored at −20 °C on a glass slide. This transfer was performed because LIBS emissions are sensitive to the state of the sample (frozen solid versus soft room-temperature). Minus 20 °C is closer to room temperature where LIBS was performed, reducing sample change with temperature change. For the thyroid, the two lobes were placed at pre-marked positions on the slide to facilitate rapid sample positioning at the laser focus. At the time of acquisition, the slide was placed on the sample holder with the right lobe at the focus, three laser pulses were fired, and the corresponding three spectra were recorded. The slide was then moved to put the left lobe at the focus and three more spectra recorded. The two slide positions on the holder were pre-marked and the laser and spectrometer were computer controlled to expedite data acquisition. Similarly for the salivary and mammary glands, three laser pulses were fired on the center of the gland on each side and the spectra recorded. Altogether, LIBS acquisition was completed approximately 60 s after removing from −20 °C to reduce sample warming.

2.3 Lithium treatment and administration

Lithium carbonate (Li_2CO_3) was purchased from Sigma Aldrich (USA). For lithium treatment, a stock solution (7.5 mM Li_2CO_3) was prepared, which was equivalent to 554 mg of Li_2CO_3 added to each liter of water. Fifty mL of the stock solution was mixed with 200 mL of water, resulting in a 1.5 mM solution of Li_2CO_3. This solution was used as the drinking water for the treated subjects. The water bottles were checked regularly and refilled to ensure the continuous supply of water. Following the same procedure, lithium solutions of 0, 0.28, 0.37, 0.55 and 1.10 ppm were prepared for immersing thyroids harvested from untreated subjects. These immersed thyroids will be used as standard samples for validating and calibrating LIBS measurements of lithium concentration in tissues. No standard reference materials are readily available that can match the matrix of the samples in this study.

2.4 Sample preparation

Thyroid and salivary glands were extracted from male subjects treated with lithium orally, modeling medical treatment. When their time point was reached (either upon entering the study or after 14, 28 or 42 days), male subjects were euthanized by 1 mL/kg body weight of 20% Dorminal via intraperitoneal injection. Each thyroid, which is positioned around the trachea (Fig. 1(b)), was extracted (Fig. 1(c)) from the treated subjects and controls. Afterwards, the salivary glands, which are located above the trachea (Fig. 1(d)), were extracted (Fig. 1(e)). The female subjects were similarly euthanized and the mammary glands, which are located on the chest and in between the forepaws (Fig. 1(f and g)), were extracted (Fig. 1(h)). Only the 42 day time point was studied for female subjects (controls and treated) as the mammary glands became sufficiently prominent for consistent extraction. All the extracted samples were rinsed using saline to remove the blood, followed by snap freezing using liquid nitrogen, and were stored in −80 °C before LIBS. The second type of samples were thyroids prepared for validating and calibrating LIBS measurements of lithium. These thyroids were immersed in 0, 0.28, 0.37, 0.55 or 1.10 ppm lithium solution for 24 hours at room temperature. After immersion, thyroids were similarly rinsed, immersed in liquid nitrogen, and stored in −80 °C before LIBS. This special calibration method was required as the samples were too small and the Li concentration too low to apply standard methods.

2.5 Data analysis

The raw data from the spectrometer was analyzed with OriginLab software. Baseline intensity was subtracted from all spectra. The spectra from the six laser pulses fired at each of the thyroid, salivary, and mammary glands were averaged to obtain three spectra (thyroid,

Biomedical Optics EXPRESS

salivary, and mammary) per subject. More pulses were not employed as the samples under study were small (~mm^2) and the expected lithium concentration was low (~ppm). Atomic emission lines were matched with elements through the Atomic Spectra Database. The intensities of the spectra were normalized by the hydrogen emission line at 656.2 nm, which is primarily due to water in the sample. T-tests were performed across the control and lithium treated subject groups using the two-tailed distribution and unpaired testing. A p-value threshold of 0.05 was considered statistically significant. Linear regression analysis was applied to compute R^2 and demonstrate a positive correlation between the sample (thyroid) lithium concentration and lithium emission intensity. The limit of detection for lithium was estimated by normalizing the lithium emission intensity from a single laser shot to the intensity of the spectral background [19]. The resulting signal to background ratio was then interpolated on the above regression line to obtain the limit of detection. Cross correlation analysis was performed to compute the correlation coefficients (cc) between the intensities of elemental emissions in the thyroid and salivary glands. Linear regression analysis was also performed between lithium intensity and that of other elements in the thyroid and salivary glands to determine the impact of tissue lithium on tissue elemental (not lithium) content.

3. Results and discussion

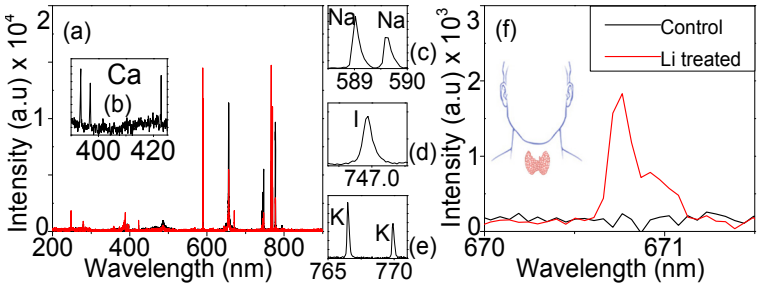

Fig. 2. (a) LIBS spectra from the thyroids of a control (black) and a 28 days lithium (Li) treated subject (red). (b) Calcium (Ca) emission lines are observed at 393.4, 396.9 and 422.7 nm in all subjects. (c) Sodium (Na) lines are at 589.0 and 589.5 nm. (d) An iodine (I) line is at 746.9 nm. (e) Potassium (K) lines are at 766.4 and 769.9 nm. (f) A Li line is observed in treated subjects only at 670.7 nm.

Figure 2(a) shows the unnormalized LIBS spectra obtained from the thyroid of a control and a 28-day lithium treated subject. There are prominent emission lines from different elements in the range of 200 to 900 nm. Calcium lines are observed at 393.4, 396.9 and 422.7 nm (Fig. 2(b)). Sodium lines are observed at 589.0 and 589.5 nm (Fig. 2(c)). An iodine line is observed at 746.9 nm (Fig. 2(d)). Potassium lines are observed at 766.4 and 769.9 nm (Fig. 2(e)). These are important elements for proper biological function. A hydrogen line is also observed at 656.2 nm, which will be used to normalize spectra. The unnormalized intensity (mean ± standard deviation) of the six shots from the control subject (Fig. 2a) for Ca, Na, I, K, and H are 404.3 ± 190.7, 4076 ± 1521, 3828 ± 1481, 5045 ± 2232 and 10240 ± 1823, respectively. For elements with multiple lines, the intensities have been averaged. Figure 2(f) is expanded for control and lithium treated subjects about 670 nm. The control spectrum does not show any emission line while the treated spectrum shows a prominent line at 670.7 nm. The Li emission line at 670.7 nm shows the accumulation of Li in the thyroid following treatment. The unnormalized intensity for lithium is 1832 ± 500 from the treated subject. Note that this and all subsequent LIBS spectra were acquired ex vivo with the sample frozen. In possible future in vivo use of LIBS, lithium and other elements can likely be detected from soft tissues, but the limits of detection will be higher.

Biomedical Optics EXPRESS

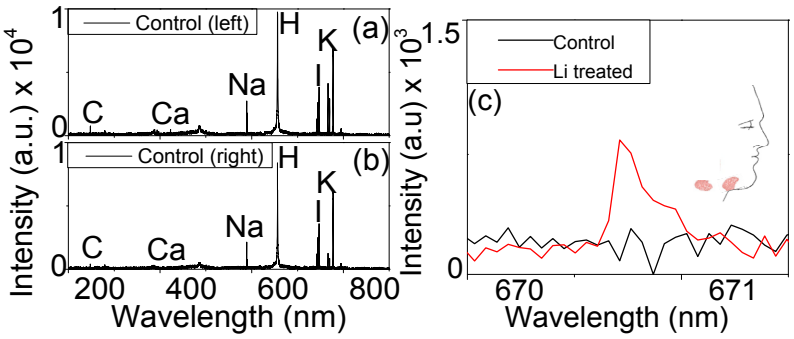

Fig. 3. (a) LIBS spectra from the (a) left and (b) right salivary glands of a control subject. Carbon (C), calcium (Ca), sodium (Na), hydrogen (H), iodine (I), and potassium (K) emission lines are observed in both glands of all subjects. (C) Li line is observed in both salivary glands (spectra averaged together) of a 42 days treated subject, but not in the control, at 670.7 nm.

Figure 3(a) and 3(b) shows the unnormalized LIBS spectra obtained from the salivary glands of a control subject. There are prominent emission lines observed from carbon at 247.6, calcium at 393.4, 396.9 and 422.7 nm, sodium at 589.0 and 589.5 nm, iodine at 746.9 nm, and potassium at 766.4 and 769.9 nm. A hydrogen line is also observed at 656.2 nm. The unnormalized intensities of the six shots from the control (left and right) for C, Ca, Na, I, K, and H are 732.2 ± 190.1, 450.6 ± 370.2, 2940 ± 774, 3624 ± 1021, 5380 ± 809 and 9760 ± 1010, respectively. Figure 3(c) is expanded for control and 28-day lithium treated subjects about 670 nm. The control spectrum does not show any emission line while the treated spectrum shows the Li line at 670.7 nm. The Li line shows the accumulation of Li in the salivary glands following treatment. The unnormalized intensity for lithium is 751 ± 419 from the treated subject.

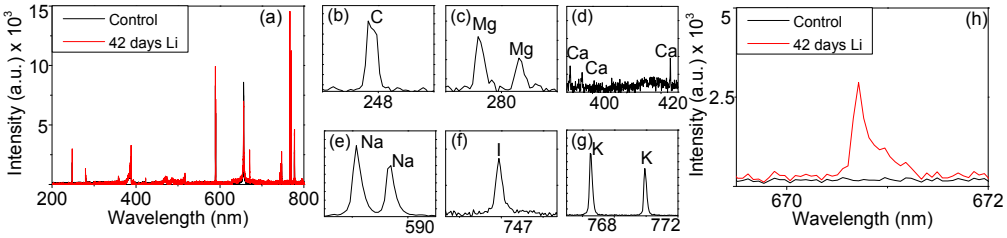

Fig. 4. (a) LIBS spectra from the mammary glands of a control (black) and a 28 days lithium treated subject (red). (b) Carbon line is observed at 247.6 nm. (c) Magnesium (Mg) lines are observed at 279.6 and 280.3 nm. (d) Calcium lines are observed at 393.4, 396.9, and 422.7 nm. (e) Sodium lines are observed at 589.0 and 589.5 nm. (f) An iodine line is observed at 746.9 nm. (g) Potassium lines are observed at 766.4 and 769.9 nm. (h) A Li line is observed in treated subjects only at 670.7 nm.

Figure 4(a) shows the unnormalized LIBS spectra obtained from the left and right mammary glands of a control and a 42-day lithium treated subject. There are prominent emission lines from different elements in the range of 200 to 800 nm. Carbon line is observed at 247.6 (Fig. 4(b)), magnesium (Mg) emission lines are observed at 279.6 and 280.3 (Fig (c)), calcium lines are observed at 393.4, 396.9 and 422.7 nm (Fig. 2(d)). Sodium lines are observed at 589.0 and 589.5 nm (Fig. 2(e)). An iodine line is observed at 746.9 nm (Fig. 2(f)). Potassium lines are observed at 766.4 and 769.9 nm (Fig. 2(g)). A hydrogen line is also observed at 656.2 nm. The unnormalized intensities (mean ± standard deviation) of the six shots from the control subject (Fig. 2a) for C, Mg, Ca, Na, I, K, and H are 3001 ± 210.2, 976 ± 151, 528 ± 181, 7045 ± 1920, 1932 ± 548, 7444 ± 2048, and 8593 ± 1925, respectively. Figure 2(h) is expanded for control and lithium treated subjects about 670 nm. The control spectrum does not show any emission line while the treated spectrum shows a prominent line

Biomedical Optics EXPRESS

at 670.7 nm. The Li emission line at 670.7 nm shows the accumulation of Li in the mammary gland following treatment. The unnormalized intensity for lithium is 2704 ± 600 from the treated subject.

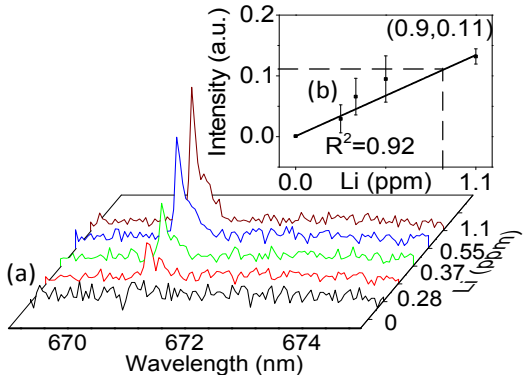

Fig. 5. (a) Normalized group averaged lithium emission lines at 670.7 nm acquired from thyroids immersed in 0 ppm lithium solution (saline only), 0.28, 0.37, 0.55, and 1.10 ppm. N = 5 for each group. Higher lithium concentration in the thyroid leads to higher LIBS intensity. (b) This is supported by linear regression analysis showing strong positive correlation between intensity and concentration (R^2 = 0.92).

Figure 5(a) shows the 670.7 nm lithium emission lines acquired from thyroids immersed in 0, 0.28, 0.37, 0.55, and 1.10 ppm lithium solution for 24 hours (N = 5 each). In 0 ppm solution (saline only), no lithium emission is observed. The immersing of thyroids in 0.28 to 1.10 ppm lithium solution progressively increases the intensity of the lithium line. Figure 5(b) presents normalized mean and standard deviation of lithium line intensity against solution lithium concentration. There is a clear trend of increasing LIBS intensity 0.03 ± 0.02 a.u. to 0.13 ± 0.01 a.u. for lithium emission obtained from thyroid immersed in lithium concentrations of 0.28 ppm to 1.1 ppm, respectively. The corresponding linear regression analysis shows a strong positive correlation (R^2 = 0.92) between lithium intensity and concentration. This data demonstrates that the 670.7 nm line belongs to lithium and that higher intensity corresponds to higher thyroid lithium concentration. This regression line is used to calibrate lithium concentrations from thyroid measurements. The data in Fig. 5 was also used to estimate the limit of detection for lithium, which is 0.12 ppm.

Figure 6(a) shows the emission lines for lithium at 670.7 nm acquired from the thyroids of untreated control subjects (N = 5), along with lines from 14 (N = 5), 28 (N = 5) and 42 (N = 5) days lithium treated subjects. The spectra have been normalized by their respective hydrogen emission lines at 656.2 nm. As expected, the control spectrum does not show lithium. The emission intensity increases considerably after 14 days on the treatment and increases further after 28 days. However, at 42 days the intensity is similar to that at 28 days, suggesting saturation. Figure 6(b) shows the iodine emission line and its intensity decreases after 14 days of treatment and holds steady through to 42 days. Figure 6(c-e) shows the calcium, sodium, and potassium emission lines, respectively. The intensities of these elemental emissions are also affected by the duration of lithium treatment.

Biomedical Optics EXPRESS

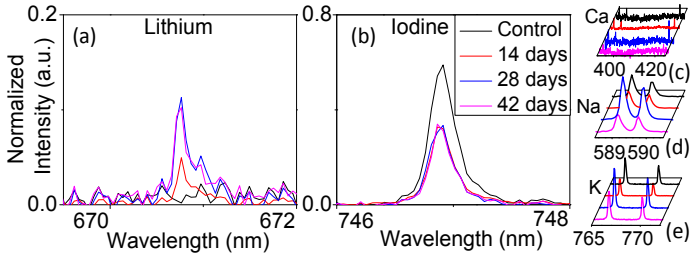

Fig. 6. Normalized group averaged LIBS spectra from the thyroids of control, 14, 28, and 42 days lithium treated subjects (N = 5 each). (a) Lithium, (b) iodine, (c) calcium, (d) sodium, and (e) potassium emission lines. The intensities have been normalized by that of the hydrogen line at 656.2 nm. Lithium treatment increases lithium intensity, but a saturation effect is seen by 28 days. In contrast, iodine intensity is decreased after 14 days of treatment and remains steady through to 42 days.

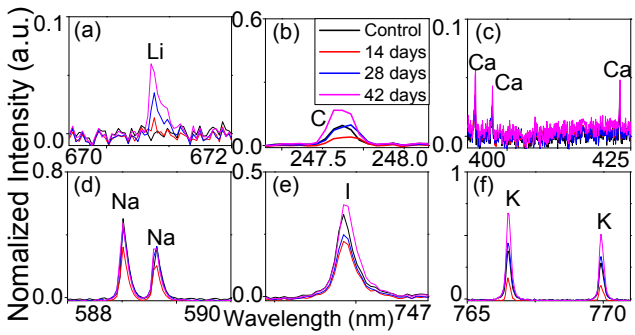

Fig. 7. Normalized group averaged LIBS spectra from the salivary glands of control, 14, 28, and 42 days lithium treated subjects (N = 5 each). (a) Lithium, (b) carbon, (c) calcium, (d) sodium, (e) iodine, and (f) potassium emission lines. Lithium treatment progressively increases lithium intensity.

Figure 7(a) shows the emission lines for lithium at 670.7 nm acquired from salivary glands of untreated control subjects (N = 5), along with lines from 14 (N = 5), 28 (N = 5) and 42 (N = 5) days lithium treated subjects. The control spectrum does not show lithium. The emission intensity increases considerably after 14 days on the treatment and increases further after 28 and 42 days on the treatment. Figure 7(b-f) shows the carbon, calcium, sodium, iodine and potassium emission lines, respectively. The intensities of these elemental emissions are also affected by the duration of lithium treatment.

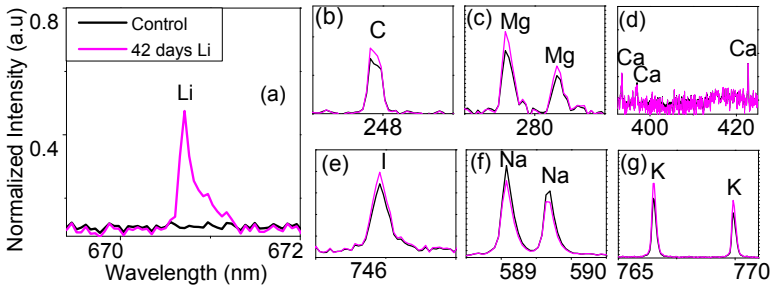

Fig. 8. Normalized and group averaged LIBS spectra from the mammary glands of control subjects (N = 5) and 42 days lithium treated subjects (N = 5). (a-g) Spectra expanded about the Li, C, Mg, Ca, Na, I and K lines, respectively. The concentrations of other elements are also affected by lithium intake.

Figure 8 shows the normalized and group averaged LIBS spectra from the mammary glands of control (N = 5) and lithium treated subjects (N = 5) after 42 days. Figure 8(a-g)

Biomedical Optics EXPRESS

shows the spectra expanded about Li, C, Mg, Ca, Na, I and K lines, respectively, from both control and lithium treated groups. One can find no lithium intensity in the averaged control group spectra. With the intake of lithium, all the elements C, Mg, Ca, Na, I and K are affected. Trace Li accumulation ($p<0.05$) in the mammary gland may affect its function and the affected mammary gland may serve as the conduit for lithium entering breast-fed infants. The further investigation of the mammary glands can help in finding lithium's effects on breast cells [20,21] and the lactation process during treatment [21,22].

Figure 9(a) shows the mean and standard deviation of thyroid lithium emission line intensities for control, 14, 28, and 42 days lithium treated subjects. The lithium intensities from 14, 28, and 42 days treated subjects are statistically significantly higher ($p<0.05$) than those from controls. The highest lithium intensity is found after 28 days of treatment (0.11 ± 0.11 a.u.). The 42 days intensity is a bit lower (0.10 ± 0.06 a.u.) and the 14 days intensity is even lower (0.04 ± 0.03 a.u.). In comparison, the intensity for controls is just 0.01 ± 0.01 a.u. These results demonstrate the accumulation of lithium in the thyroid during lithium treatment. Applying the regression line from Fig. 5 to the thyroid lithium measurements from treated subjects, the lithium concentrations at 14, 28, and 42 days are approximately 0.4, 0.9, and 0.8 ppm, respectively. With intrathyroidal lithium accumulation, the concentrations of other elements are affected. Figure 9(b) shows the iodine emission intensity. The iodine intensity in controls is statistically higher ($p<0.001$) than those in 14, 28, and 42 days treated subjects. Interestingly, the intensity drop with treatment is considerable at 14 days but holds steady through to 42 days.

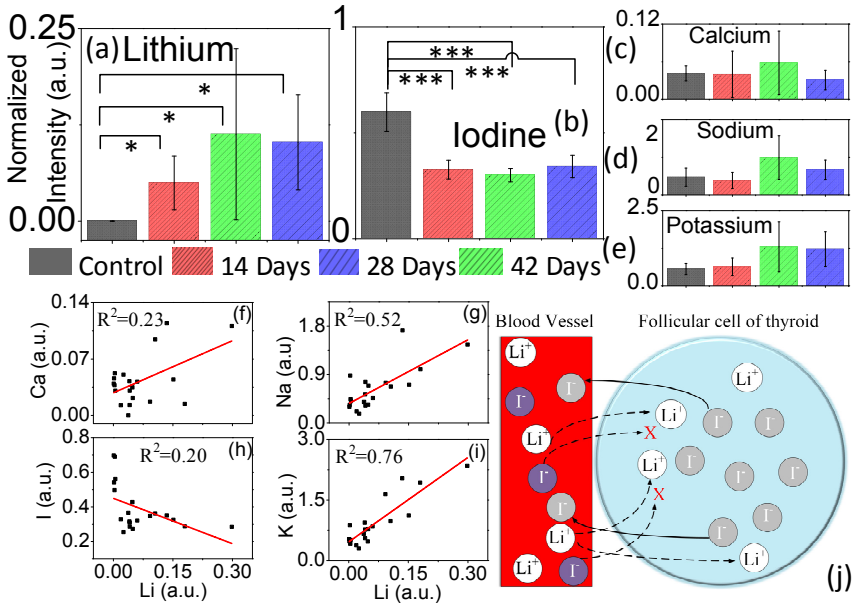

Fig. 9. Bar plots showing the mean and standard deviation of emission intensities from the thyroids of control, 14, 28, and 42 days lithium treated subjects. (a) Lithium, (b) iodine, (c) calcium, (d) sodium, and (e) potassium lines. Intensities have been normalized by the 656.2 nm hydrogen line intensity. Statistical analysis across groups was performed with the standard two-tailed t-test with p-value threshold of 0.05 considered statistically significant. * indicates $p<0.05$ and *** indicates $p<0.001$. The multiple linear regression analyses between lithium intensity and that of calcium (f), sodium (g), iodine (h) and potassium (i). (j) Illustration of lithium ions entering a thyroid follicular cell and preventing iodine ions from entering.

The cross correlation analysis suggests that lithium emission intensity in thyroid is negatively correlated with that of iodine (cc = −0.5). This agrees with Figs. 6 and 9 and quantifies that intrathyroidal iodine is reduced when intrathyroidal lithium increases. In contrast, thyroid calcium, sodium, and potassium emission intensities (Fig. 9(c-e)) are

Biomedical Optics EXPRESS

positively correlated with lithium intensity (see Table 1 for details). This means that in general, lithium accumulation increases intrathyroidal calcium, sodium, and potassium. The multiple linear regression analyses similarly demonstrate an inverse relationship between intrathyroidal lithium and iodine, and a positive relationship between lithium and calcium, sodium, and potassium (see Fig. 9(f-i)). The changes in intrathyroidal concentrations of these key elements during lithium treatment can negatively influence the synthesis of thyroid hormones. This in turn can lead to a range of thyroid disorders, including hypo and hyperthyroidism. It is interesting to note that such thyroid disorders have been extensively reported in patients receiving lithium treatment for mental disorders [23].

Table 1. Cross correlation coefficients between elemental emission intensities measured from the thyroid.

	Ca	Na	I	K	Li
Ca	1.00	0.64	0.01	0.49	0.49
Na	-	1.00	–0.28	0.90	0.72
I	-	-	1.00	–0.38	–0.50
K	-	-	-	1.00	0.84
Li	-	-	-	-	1.00

Figure 9(j) hypothesizes the mechanism through which lithium treatment reduces intrathyroidal iodine. During treatment, lithium ions enter the thyroid follicular cells. Lithium may enter through the sodium/potassium ion channel as they all exist as positive ions. Accumulation of lithium ions in the follicular cell may limit the iodide influx from the blood vessel to the cell [24] and increases the sodium and potassium ion concentration [25]. This reduction of iodine due to accumulation of lithium may be related to tyrosine increase with lithium treatment [26]. This tyrosine accumulation in the thyroid likely indicates an inability to convert tyrosine into T3 and T4 hormones due to the lack of iodine, leading to thyroid dysfunction.

Figure 10(a) shows the mean and standard deviation of lithium emission line intensities from salivary glands of control, 14, 28, and 42 days lithium treated subjects. The lithium intensities steadily increase from 14 to 28 and 42 days. The intensities in treated subjects are statistically significantly greater than those in controls ($p<0.05$). The highest lithium intensity is found after 42 days of treatment. Salivary gland calcium, iodine, and potassium emission intensities are positively correlated with lithium intensity, while sodium is negatively correlated (see Table 2 for details). The multiple linear regression analyses for salivary gland similarly show that Ca, I and K intensities are positively related to that of lithium, while sodium is inversely related (Fig. 10(g-j)). These results demonstrate the accumulation of lithium in the salivary gland during lithium treatment. With lithium accumulation in salivary gland, the concentrations of other elements are affected (Fig. 10(b-f)). Clinically, lithium ions have been detected in the saliva of patients treated with lithium [27].

Biomedical Optics EXPRESS

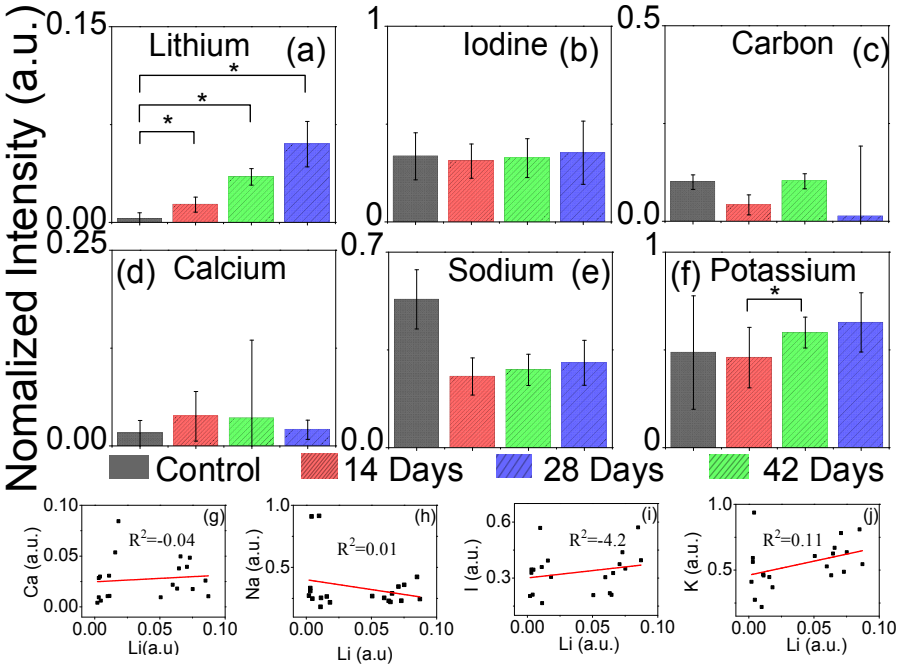

Fig. 10. Bar plots showing the mean and standard deviation of emission lines from the salivary glands of control, 14, 28, and 42 days lithium treated subjects. (a) Lithium, (b) iodine, (c) carbon, (d) calcium, (e) sodium, and (f) potassium lines. * indicates $p<0.05$. The multiple linear regression analyses between lithium intensity and that of calcium (g), sodium (h), iodine (i) and potassium (j).

Table 2. Cross correlation coefficients between elemental emission intensities measured from the salivary gland.

	Ca	Na	I	K	Li
Ca	1.00	–0.17	0.11	0.11	0.11
Na	-	1.00	0.28	0.21	–0.25
I	-	-	1.00	–0.10	0.23
K	-	-	-	1.00	0.40
Li	-	-	-	-	1.00

4. Conclusion

In conclusion, laser-induced breakdown spectroscopy has been developed to detect trace levels of lithium in biological tissues. Lithium emissions were observed at 670.7 nm from rat thyroid, salivary, and mammary glands. The emission intensity increased with tissue lithium concentration. The highest lithium concentration measured from the thyroid of lithium treated subjects was approximately 0.9 ppm. With the intrathyroidal increase in lithium, intrathyroidal iodine was reduced. The reduction of this biologically critical element, along with changes in the concentrations of other key elements such as sodium, calcium, and potassium, may impair the production of T_3 and T_4 hormones. Lithium observed in the salivary and mammary glands are likely related to lithium observations in saliva and breast milk, respectively. This study provides a novel method to rapidly detect lithium in tissues in situ, along with naturally occurring, biologically important elements. Going forward, LIBS can be employed to study lithium biodistribution in other affected organs, such as the kidneys, and at the cellular level. Further, this optical method can potentially be extended to in vivo and human measurements.

Biomedical Optics EXPRESS

Funding

City University of Hong Kong (project numbers 7200414, 9610338, and 9610378).

Disclosures

The authors declare that there are no conflicts of interest related to this article.